Hindawi
International Journal of Intelligent Systems
Volume 2024, Article ID 4541163, 16 pages
https://doi.org/10.1155/2024/4541163

WILEY | Hindawi

Research Article

Enhanced Multiobjective Optimization Algorithm for Intelligent Grid Management of Renewable Energy Sources

Xue Han,[1] **JiKe Ding**,[1] **and Honglin Cheng**[2]

[1]*Xuzhou Open University, College of Information Engineering, Xuzhou 221000, China*
[2]*Xuzhou University of Technology, School of Information Engineering, Xuzhou 221000, China*

Correspondence should be addressed to Xue Han; snow@xzit.edu.cn

Received 1 September 2023; Revised 19 November 2023; Accepted 22 December 2023; Published 2 January 2024

Academic Editor: Said El Kafhali

Optimal scheduling of microgrids (MGs) is a crucial component of smart grid optimization, playing a vital role in minimizing energy consumption and environmental degradation. However, existing methods tend to consider only a single optimization and do not consider the multiobjective optimization problem of MGs in a comprehensive and integrated way. This study proposes a comprehensive multiobjective optimal scheduling methodology for renewable energy MGs, incorporating demand-side management (DSM) considerations. Initially, a DSM multiobjective optimization model is formulated, focusing on the load shifting of controllable devices within the MG to refine the electricity consumption structure. This model contemplates the renewable energy consumption of the MG, customer electricity purchase costs, and load smoothness. Subsequently, a multiobjective optimization model for grid-connected MGs, encompassing wind and photovoltaic power generation, is constructed with the dual objectives of economic and environmental optimization for the MG. Ultimately, a multimodal multiobjective optimization algorithm, amalgamating a local convergence index and an environment selection strategy, is proposed to solve the model. The experimental results show that compared with other methods, the proposed method in this paper can reduce the integrated cost by 32.6% and 38.9% in summer and 19.4% and 40.2% in winter. This stands out as a unique contribution in the field of MG optimization, as it integrates DSM considerations into a multiobjective optimization model. This methodology achieves a balance between minimizing energy consumption and environmental degradation while also enhancing economic efficiency.

1. Introduction

In the contemporary era, the exhaustion of conventional energy sources, such as coal, is escalating, engendering a mounting energy crisis [1]. Concurrently, there is a rapid economic development, technological advancement in power plants, and a steady surge in electricity consumption among Chinese residents [2]. The power grid's role extends beyond merely supplying electricity to households; it encompasses ensuring the quality, safety, and reliability of power transmission. Nonetheless, the grid is afflicted by numerous deficiencies requiring rectification. In remote and thinly populated regions, long-distance power generation is impractical, inflating transportation costs and squandering resources. Although constructing new power plants in these areas could remedy the issue, the prolonged construction duration and exorbitant costs render this solution unfeasible.

Coal predominates as the principal power generation source, yet coal reserves are progressively diminishing year by year [3]. Hence, integrating new green energy sources and seamlessly connecting their power generation networks to the larger grid could effectively address the high-power consumption dilemma in remote residential areas [4]. An off-grid hybrid solar PV/fuel cell power system is designed and optimized for a desert residential community, employing an integrated modeling, simulation, and optimization approach. The study investigates the impact of temperature and dust on solar PV panels, with the goal of increasing renewable energy penetration, reducing greenhouse gas emissions, and minimizing energy costs [5]. To mitigate the energy deficiency, researchers have shifted their

focus towards cleaner, greener energy alternatives. Investigating these energy sources renders our energy generation technology more cost-effective and reliable, culminating in the inception of distributed generation (DG) in this societal context [6].

In recent years, the DG concept has gained widespread recognition, offering unique benefits, such as flexible installation, high reliability, and superior energy efficiency. The system is strategically situated near the distribution grid or load (typically below 30 MW) to bolster the larger grid's economic operation. However, several unresolved challenges plague the DG system, the most pivotal being its uncontrollability relative to the grid [7]. The excessive consumption induced by a single microsource connected to the grid hinders the full-fledged development of DG. Additionally, the DG system may induce voltage and frequency fluctuations in the grid during connection, deteriorating power quality and compromising the grid's security and reliability [8]. To address these issues comprehensively, the MG concept was proposed, enabling DG to maximize its advantages and potential in integrating large-scale DG power sources into the grid. MGs amalgamate DG power supplies, energy storage apparatuses, energy conversion devices, loads, protection mechanisms, and detection instruments into a compact power generation and distribution system. This architecture facilitates autonomous control, self-protection, and self-management. The MG can function autonomously as a module interconnected with the larger grid, denoted as grid-connected operation, or independently as a self-contained entity, referred to as islanded operation [9]. Within the MG, each internal device is meticulously configured to furnish power to the MG's minor loads and judiciously modulate the internal voltage frequency and power to ascertain the unimpeded functioning of the MG's internal components. Conversely, the MG's external segment is governed as a discrete system by the expansive grid distribution. The advent of MGs smoothes the grid's development, compensates for traditional DG's limitations, and stipulates superior benchmarks and prerequisites for actualizing smart grid infrastructure [10].

The advent of MGs facilitates resolving the discord between distributed energy and the grid while optimizing the merits of DG and rectifying traditional DG's shortcomings. MG's optimal scheduling allows for the strategic management of DG power outputs and the regulation of transmission power between the MG and the main grid. This orchestration is designed to achieve multiple goals, including cost and emissions reduction, as well as enhanced reliability and generation efficiency [11]. To optimize MG operation and fully harness its benefits, it is imperative to conduct thorough research on its optimal control strategies.

For MG optimization dilemmas, employing multiobjective models renders the system more holistic and efficacious [12]. Numerous studies have been undertaken to address MGs' multiobjective optimization challenges. To preserve the environment, demand response models [13] have been devised to furnish potential infrastructures that concurrently enhance efficiency and reduce energy consumption. Some researchers have implemented the distributed gradient algorithm (DGA) to tackle the distributed sum optimization (DSO) problem [14]. With artificial intelligence's evolution, a plethora of intelligent algorithms have emerged. Zhang et al. [15] proposed a multiobjective fireworks algorithm (MOFWA) to optimally address the multimobile charging planning problem. Younes et al. [16] employed an artificial bee colony (ABC) algorithm to ascertain the optimal configuration results for the MG system's total operating cost. Zhu et al. [17] proposed a multiobjective gray wolf optimization algorithm (GWO) based on the multiobjective Gray Wolf optimization algorithm (MOGWO). Nevertheless, these algorithms have high computational complexity and scalability issues, which are crucial for their implementation in the real world, especially in large-scale MG systems. Vosoogh et al. [18] formulated an optimal probability model for MG energy management, considering multifactor uncertainty using the 2 m point estimation method. Al-Tameemi et al. [19] combined the GWO and particle swarm optimization (PSO) algorithms to determine the optimal size and pollution minimization optimization results for different system components. Ghiasi [20] employed multiobjective particle swarm optimization in an intelligent approach. This approach conducted a thorough analysis of the new structure of alternating current (AC) and direct current (DC) systems. Subsequently, it determined the capacity and optimal design of hybrid renewable energy sources in smart microgrid (MG). Some researchers proposed and implemented an improved multiobjective differential evolution (IMODE) optimization algorithm for generation scheduling in smart MG systems while considering economics and emissions as competing issues [21]. These studies rely heavily on simulations or theoretical models. The absence of real-world validation or case studies diminishes the practical applicability of the proposed algorithms and their relevance to actual MG systems. Some other researchers presented an enhanced control strategy for renewable energy resources connected to the grid through voltage-sourced converters (VSCs) in MGs [22]. However, these studies do not adequately address the dynamic nature of MGs, such as varying energy demand patterns, fluctuating renewable energy sources, and real-time operational changes.

Globally, MG development is advancing towards maturity, with exceptionally developed MGs established in Europe and the United States. Europe, the pioneer in proposing "smart power networks," steers its research endeavors toward energy, environmental conservation, and sustainable development [23]. These investigations encompass control, analysis, optimization, forecasting, multi-MG systems, and MGs' economic dispatch [24]. For instance, the National Technical University of Athens (NTUA) MG is primarily engineered to scrutinize MG control strategies, mode switching operations, energy scheduling based on economic considerations, and the analysis and optimization of multilayered control structures for MGs. The Demotec MG cluster control framework, devised by the University of Kassel's Institute of Photovoltaic in Germany, comprises multiple sub-MG network systems [25]. This structure allows comprehensive reconfiguration and optimization of the entire MG. It facilitates seamless

transitions between multiple subgrid networks and islanding modes. Additionally, it assesses the impact of load fluctuations on grid stability by incorporating or excluding diverse load bursts [26]. The Labein MG in Spain's Basque Country concentrates on scheduling tactics and communication protocols for multiple MGs, centralized and decentralized control strategies for nonislanded operations, and tariff trading in a novel electricity market under MGs [27]. Lastly, the CESI MG in Milan, Italy, was investigated by integrating diverse generation devices and energy storage mechanisms, while optimizing the network's communication topology to actualize optimal MG control and conduct comprehensive power quality analysis by leveraging multiple communication methods [28].

The abovementioned algorithms used in the existing model solution are relatively single, which may result in the lack of global search and optimization ability in integrated energy system energy optimization and management. The lack of global or local optimal solutions in practical applications may lead to a lack of overall understanding of the problem by decision makers, resulting in unnecessary difficulties or economic losses. Most of the multiobjective optimization algorithms only focus on obtaining as many global optimal solutions as possible but neglect the search for local optimal solutions. However, the research on this kind of problem is still relatively limited and the research on this kind of problem is still in the early stage.

This paper studies how to optimize the control of MG power load under the condition of maintaining the safe and stable operation of MG system, so as to maximize the economic and environmental benefits of MG. To augment the new energy consumption of MG and thereby enhance its operational efficiency, this study initially constructs a DSM multiobjective optimization model grounded in smart grid principles to refine the load structure. Subsequently, a multiobjective optimal dispatching model for renewable energy MG is developed, focusing on economic and environmental protection objectives. Ultimately, a multimodal multiobjective optimization algorithm is employed to ascertain global and local optimal solution sets to resolve the model. The proposed MG dispatching model's efficacy is corroborated through simulation analysis in a representative MG scenario.

The key features and main contributions of the multimodal multiobjective optimization algorithm are as follows:

(1) DSM integration: our algorithm incorporates DSM principles, aligning it with the smart grid paradigm. This integration enables the refinement of load structures and enhances energy consumption efficiency.

(2) Multiobjective optimization: the algorithm is designed to address both economic and environmental objectives, acknowledging the need to balance economic efficiency and environmental protection in MG operations.

(3) Global and local optimal solutions: our algorithm is equipped to determine global and local optimal solution sets. This feature enhances the robustness of the optimization process, ensuring a comprehensive exploration of potential solutions.

This paper consists of six main parts. Section 1 is the introduction, Section 2 is the demand-side management multiobjective optimization model, Section 3 is the new energy MG economic environment optimization dispatch model, Section 4 is the multimodal multiobjective optimization solution model based on local convergence index, Section 5 is the result analysis and discussion, and Section 6 is the conclusion.

2. Demand-Side Management Multiobjective Optimization Model

This paper adopts the DSM strategy based on load shifting of controllable power equipment in MG to achieve optimal control of MG power consumption load. The DSM multiobjective optimization model is established with the objectives of improving the new energy consumption, reducing the cost of electricity purchase by customers smoothing the load, and taking the electricity demand of multiple controllable devices as the constraints.

2.1. Objective Functions

2.1.1. Objective Function 1: Maximizing New Energy Consumption. The access of demand-side controllable equipment is controlled with the optimization objective of improving new energy consumption. When wind power and photovoltaic power generation are insufficient, the electricity consumption load is reduced, and when power generation is sufficient, the load is increased. This can improve the suitability of MG load and new energy generation. The optimization objective function F_1 is shown as follows:

$$F_1 = \frac{1}{\sum_{n=1}^{\tau} \min\left(\left(\mathrm{UL}(n)/R(n)\right), 1\right)}, \tag{1}$$

where τ is the total number of time intervals divided by 1 d; $\mathrm{UL}(n)$ is the actual customer load at moment n; and $R(n)$ is the sum of the predicted power output of the scenery at moment n. From (1), it can be seen that the higher the utilization rate of new energy the smaller the value of $F1$.

2.1.2. Objective Function 2: Load Management for Cost Reduction. The DSM strategy reduces the access to electricity-using equipment in the peak period and increases the access to electricity-using equipment in the low period. This can reduce the cost of electricity for customers and smooth the electricity load curve. The optimization objective function F_2 is shown as follows:

$$F_2 = \sum_{n=1}^{\tau} \mathrm{UL}(n) \cdot u(n), \tag{2}$$

where $u(n)$ is the price of electricity at moment n.

2.1.3. Objective Function 3: Ensuring Load Stability. Since the electricity price is high in the peak period and low in the trough period, F_2 will lead to a decrease in electricity consumption in the peak period and an increase in electricity consumption in the trough period. In order to prevent peak-valley interchange, using the load peak-valley difference as the objective function can ensure the smoothness of the electricity consumption load. The optimization objective function F_3 is shown as follows:

$$F_3 = \max(\mathrm{UL}) - \min(\mathrm{UL}). \tag{3}$$

The actual user load $\mathrm{UL}(n)$ at moment n in the 3 objective functions consists of uncontrollable and controllable loads, and its mathematical expression is as follows:

$$\mathrm{UL}(n) = \mathrm{FL}(n) + \mathrm{CL}(n) - \mathrm{DL}(n), \tag{4}$$

$$\begin{aligned}\mathrm{CL}(n) = &\sum_{l=1}^{L}\sum_{s=n-w_l}^{n-1} T_{lsn}\cdot U_{l1} \\ &+ \sum_{l=1}^{T}\sum_{z=1}^{d_l-1}\sum_{s=n-z-w_l}^{n-z-1} T_{ls(n-z)}\cdot U_{l(z+1)},\end{aligned} \tag{5}$$

$$\begin{aligned}\mathrm{DL}(n) = &\sum_{l=1}^{L}\sum_{s=n+1}^{n+w_l} T_{ls}\cdot U_{l1} \\ &+ \sum_{l=1}^{T}\sum_{z=1}^{d_l-1}\sum_{s=n-z+1}^{n-z+w_l} T_{l(n-z)s}\cdot U_{l(z+1)},\end{aligned} \tag{6}$$

where $\mathrm{FL}(n)$ is the load forecast at moment n; $\mathrm{CL}(n)$ is the controllable load connected at moment n; and $\mathrm{DL}(n)$ is the controllable load transferred out at moment n. L is the type of controllable equipment and w_l is the maximum transfer time of the l-th controllable equipment. T_{lsn} is the amount of equipment of the l-th controllable equipment transferred from moment s to moment n. T_{lns} is the amount of equipment of the l-th controllable equipment transferred from moment n to moment s. $T_{ls(n-z)}$ is the amount of equipment of the l-th controllable equipment transferred from moment s to moment $(n-z)$. $T_{l(n-z)s}$ is the number of devices of the l-th controllable device transferred from moment $(n-z)$ to moment s. U_{l1} is the load of the l-th controllable device at the start moment. $U_{l(z+1)}$ is the load of the l-th controllable device at the $(z+l)$ moment. d_l is the time of the required load of the l-th controllable device.

2.2. Constraint Conditions. Considering the actual load shifting situation and the limitation of the power demand of controllable devices, the DSM multiobjective optimization problem described needs to satisfy the following constraints.

2.2.1. Constraint Condition 1: Nonnegative Device Shifting. The number of controllable devices shifted at any moment is nonnegative.

$$T_{ls} \geqslant 0. \tag{7}$$

2.2.2. Constraint Condition 2: Device Quantity Limit. The number of controllable devices does not exceed the total number.

$$\sum_{l=1}^{L} T_{\mathrm{lsn}} \leqslant TC(s), \tag{8}$$

where $\mathrm{NC}(s)$ is the total number of controllable devices with power demand at the moment s.

2.2.3. Constraint Condition 3: Minimum Connection Time. Each controllable device is connected for more than the required time to disconnect.

$$U_{l(n-z+1)} = 0, \quad \forall (n-z+1) > d_l, \tag{9}$$

where $U_{l(n-z+1)}$ is the load of the l-th controllable equipment at the moment of $(n-z+1)$.

2.2.4. Constraint Condition 4: Device Shifting Sequence. Controllable equipment loads can only be moved forward in time, adhering to a specific sequence, and the transfer duration must not exceed the predetermined limit.

$$T_{lsn} = 0, \quad \forall s > n, \tag{10}$$

$$T_{\mathrm{ln}} = 0, \quad \forall (n-s) > w_l. \tag{11}$$

Under the constraints of equations (7)–(11), the $\min\{F_1, F_2, F_3\}$ problem is solved with the number of accesses of controllable devices at each moment in 1 d as the decision variable. This yields the real load profile that satisfies the desired target with the participation of user-side controllable devices and the accesses of controllable devices within the MG at different moments in 1 d.

3. New Energy MG Economic Environment Optimization Dispatch Model

This paper establishes a new energy MG model as shown in Figure 1, includes wind turbine (WT), photovoltaic (PV), diesel generator (DE), microturbine (MT), batteries (BAT), and controllable loads. The MG is connected to the grid through a main isolator and can purchase power from the grid when MG capacity is insufficient. The dispatch model of this MG is developed with the optimization objectives of economy and environmental friendliness.

3.1. Objective Functions

3.1.1. Objective Function 1: Economic Efficiency Objective. To improve the economic efficiency of station MG operation, the economic objective of station MG dispatch is expressed by the operating cost C_{opt} of station MG. It includes the fuel cost of traditional distributed power sources, the operation and maintenance cost of distributed power sources and energy storage systems, and the cost of station area MGs interacting with the larger grid through contact lines. This paper optimizes the decision variables, such as the

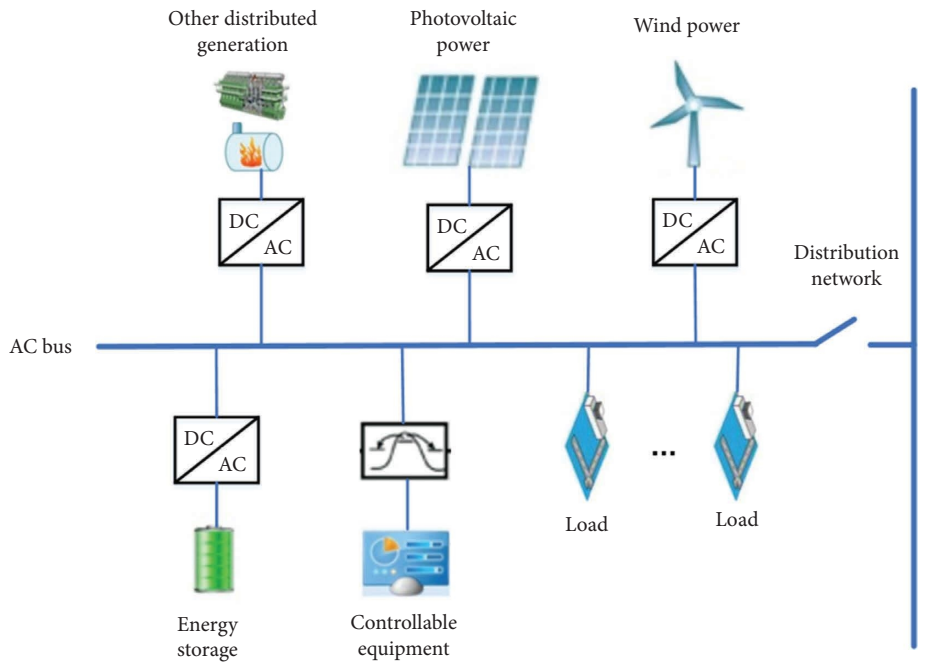

Figure 1: Schematic diagram of MG composition.

output power of distributed power sources and the charging/discharging power of the energy storage system, to minimize C_{opt}. The optimization objective C_{opt} is expressed as follows:

$$C_{\text{opt}} = \sum_{n=1}^{N} \left(\sum_{x=1}^{T_a} \left(C_{\text{fuel},y}(n) + C_{\text{om},y}(n) \right) + C_{\text{grid}}(n) \right), \tag{12}$$

where T_a is the number of DGs in the MG and N is the total number of time intervals divided by 1 d. $C_{\text{fuel},y}(n)$ is the fuel cost of the y-th DG at moment n. $C_{\text{om},y}(n)$ is the operation and maintenance cost of the y-th DG at moment n. $C_{\text{grid}}(n)$ is the cost of the MG's interaction with the larger grid at moment n.

The fuel cost of the MG is specifically expressed as follows:

$$C_{\text{fuel},y}(n) = C_{\text{MT}f,y}(n) + C_{\text{DEf},y}(n),$$

$$\begin{cases} C_{\text{MT}f} = C \dfrac{1}{LHV} \dfrac{U_{\text{MT}}}{\eta_{\text{MT}}}, \\ \eta_{\text{MT}} = 0.0753 \left(\dfrac{U_{\text{MT}}}{65} \right)^3 - 0.3095 \left(\dfrac{U_{\text{MT}}}{65} \right)^2 \\ \quad + 0.4174 \left(\dfrac{U_{\text{MT}}}{65} \right) + 0.1068, \end{cases} \tag{13}$$

$$C_{\text{DEf}} = \alpha + \beta U_{DE} + \gamma U_{DE}^2,$$

where C_{MTf} is the fuel cost of MT; C is the unit price of natural gas. LHV is the low heating value of natural gas. U_{MT} is the output power of MT. η_{MT} is the output efficiency of MT; C_{DEf} is the fuel cost of DE; and U_{DE} is the output power of DE. α, β, γ are the fuel cost coefficients of DE.

The O&M cost of power equipment in MG is usually related to the output power of power equipment, and the calculation formula is shown in equations (14) and (15).

$$C_{om,y}(n) = \zeta_y U_{DG,y}(n), \tag{14}$$

$$C_{om} = \sum_{n=1}^{N} \sum_{y=1}^{T_a} C_{om,y}(n), \tag{15}$$

where ζ_y is the operation and maintenance cost factor of the y-th DG. $U_{\text{DG},y}(n)$ is the output power of the jth DG at time n.

MG operates in the grid-connected state and purchases power from the larger grid when the generation unit is under-generated, and the interaction cost at this time is as follows:

$$C_{\text{grid}}(n) = C_{\text{buy}}(n) U_{\text{grid}}(n), \tag{16}$$

where $C_{\text{buy}}(n)$ is the price of electricity purchased by the MG from the larger grid at moment n. $U_{\text{grid}}(n)$ is the power of interaction between the MG and the larger grid at moment n.

3.1.2. Objective Function 2: Environmental Objective. The treatment cost C_{plut} of the total amount of polluting gases emitted by the new energy MG is used as the environmental cost to make it as small as possible. This paper considers the coefficients of pollutant gases emitted by various sources and optimizes the decision variables to minimize C_{plut}. The optimization objective C_{plut} is expressed as follows:

$$C_{\text{plut}} = \sum_{n=1}^{N}\left(\sum_{r=1}^{T_e}\zeta_r\left(\sum_{j=1}^{T_a} e_{\text{DG},y,r}U_{\text{DG},y}(n)\right)\right) + \sum_{n=1}^{N}\left(\sum_{r=1}^{T_e}\zeta_r\left(e_{\text{BAT},r}U_{\text{BAT}}(n)\right)\right) + \sum_{n=1}^{N}\left(\sum_{r=1}^{T_e}\zeta_r\left(e_{\text{grid},r}U_{\text{grid}}(n)\right)\right), \tag{17}$$

where T_e is the pollutant gas type. $e_{\text{DG},y,r}$, $e_{\text{BAT},r}$, and $e_{\text{grid},r}$ are the coefficients of the y-th DG, energy storage system, and the r-th pollutant gas emitted from the large grid, respectively. $U_{\text{BAT}}(n)$ is the output power of the energy storage system at moment n. $U_{\text{grid}}(n)$ is the output power of the large grid at moment n. ζ_r is the treatment cost coefficient of the r-th pollutant gas.

3.2. Constraint Conditions

3.2.1. Constraint Condition 1: Tidal Current Constraint.

$$\sum_{y=1}^{T_a} U_{\text{DG},y}(n) + U_{\text{BAT}}(n) + u_{\text{grid}}(n) + U_{\text{new}}(n) = U_{\text{Load}}(n), \tag{18}$$

where $U_{\text{new}}(n)$ and $U_{\text{Load}}(n)$ are the new energy generation power and total load of users at time n, respectively.

3.2.2. Constraint Condition 2: Power Constraint of DG and Large Grid Output.

$$U_{\text{DG},y}^{\min} \leqslant U_{\text{DG},y}(n) \leqslant U_{\text{DG},y}^{\max}, \tag{19}$$

$$U_{\text{grid}}^{\min} \leqslant U_{\text{grid}}(n) \leqslant U_{\text{grid}}^{\max}, \tag{20}$$

where $U_{\text{DG},y}^{\min}$ and $U_{\text{DG},y}^{\max}$ are the lower and upper limits of the output of the y-th DG, respectively. $U_{\text{grid}}^{\min}$ and $U_{\text{grid}}^{\max}$ are the lower and upper limits of the output of the large grid, respectively.

3.2.3. Constraint Condition 3: Climbing Constraint of DG and Large Grid Output

$$\Delta U_{\text{DG},y}^{\text{dn}} \leqslant U_{\text{DG},y}(n) - U_{\text{DG},y}(n-1) \leqslant \Delta U_{\text{DG},y}^{\text{up}}, \tag{21}$$

$$\Delta U_{\text{grid}}^{\text{dn}} \leqslant U_{\text{grid}}(n) - U_{\text{grid}}(n-1) \leqslant \Delta U_{\text{grid}}^{\text{up}}, \tag{22}$$

where $\Delta U_{\text{DG},y}^{\text{dn}}$ and $\Delta U_{\text{DG},y}^{\text{up}}$ are the downhill and uphill constraints of the y-th DG, respectively. $\Delta U_{\text{grid}}^{\text{dn}}$ and $\Delta U_{\text{grid}}^{\text{up}}$ are the downhill and uphill constraints of the large grid, respectively. $U_{\text{DG},y}(n-1)$ is the output power of the y-th DG at the moment $n-1$. $U_{\text{grid}}(n-1)$ is the output power of the large grid at the moment t-1.

3.2.4. Constraint Condition 4: Energy Storage System Operation Constraint

$$\begin{cases} E_{\text{BAT}}^{\min} \leqslant E_{\text{BAT}}(n) \leqslant E_{\text{BAT}}^{\max}, \\ \eta_{\text{ch}}U_{\text{ch}}(n) \leqslant \min\left(U_{\text{ch}}^{\max}, E_{\text{BAT}}^{\max} - E_{\text{BAT}}(n-1)\right), \\ E_{\text{BAT}}(n-1) - E_{\text{BAT}}^{\min} \leqslant \dfrac{P_{\text{dch}}(n)}{\eta_{\text{dch}}} \leqslant P_{\text{dch}}^{\max}, \\ \sum_{n=1}^{N}\eta_{\text{ch}}U_{\text{ch}}(n) = \sum_{n=1}^{N}\dfrac{U_{\text{dch}}(n)}{\eta_{\text{dch}}}, \end{cases} \tag{23}$$

where $E_{\text{BAT}}(n)$, $E_{\text{BAT}}^{\min}$, and $E_{\text{BAT}}^{\max}$ are the lower and upper limits of energy storage capacity and energy storage capacity at moment n, respectively. $U_{\text{ch}}(n)$ and $U_{\text{dch}}(n)$ are the charging and discharging power at moment n, respectively. $U_{ch}^{\max}$ and $U_{\text{dccx}}^{\max}$ are the maximum values of charging and discharging power, respectively. η_{ch} and η_{dch} are the charging and discharging efficiency of the energy storage system, respectively.

3.2.5. Constraint Condition 5: Rotating Standby Constraint

$$\begin{cases} \sum_{j=1}^{T_a} R_y^{\text{up}}(n) + R_{\text{grid}}^{\text{up}}(n) + E_{\text{BAT}}(n) - E_{\text{BAT}}^{\min} \geqslant R_{\text{sys}}^{\text{up}}(n), \\ R_y^{\text{up}}(n) = \max\left(U_{\text{DG},y}^{\max} - U_{\text{DG},j}(n), \Delta U_{\text{DG},y}^{\text{up}}\right), \\ R_{\text{grid}}^{\text{up}}(n) = \max\left(U_{\text{grid}}^{\max} - U_{\text{grid}}(n), \Delta U_{\text{grid}}^{\text{up}}\right), \\ \sum_{y=1}^{T_a} R_y^{\text{dn}}(n) + R_{\text{grid}}^{\text{dn}}(n) + E_{\text{BAT}}^{\max} - E_{\text{BAT}}(n) \geqslant R_{\text{sys}}^{\text{dn}}(n), \\ R_y^{\text{dn}}(n) = \max\left(U_{\text{DG},y}(n) - U_{\text{DG},y}^{\min}, \Delta U_{\text{DG},y}^{\text{dn}}\right), \\ R_{\text{grid}}^{\text{dn}}(n) = \max\left(U_{\text{grid}}(n) - U_{\text{grid}}^{\min}, \Delta U_{\text{grid}}^{\text{dn}}\right), \end{cases} \tag{24}$$

where $R_y^{\text{up}}(n)$ and $R_y^{\text{dn}}(n)$ are the climbing capacity available from the y-th DG at time n. $R_{\text{grid}}^{\text{up}}(n)$ and $R_{\text{grid}}^{\text{dn}}(n)$ are the climbing capacity available from the large grid. $R_{\text{sys}}^{\text{up}}(n)$ and $R_{\text{sys}}^{\text{dn}}(n)$ are the positive rotating standby demand and negative rotating standby demand of the system at time t, respectively.

Under the constraints of equations (19)–(25), the multiobjective optimization problem of $\min\{C_{\text{opt}}, C_{\text{plut}}\}$, which is the mathematical model of MG dispatch. The optimization includes variables at each MG 1 d time period: output power of distributed sources, energy storage system charging/discharging power, and power purchased from the larger grid by MG. The flow diagram of new energy MG scheduling with DSM in this paper is shown in Figure 2.

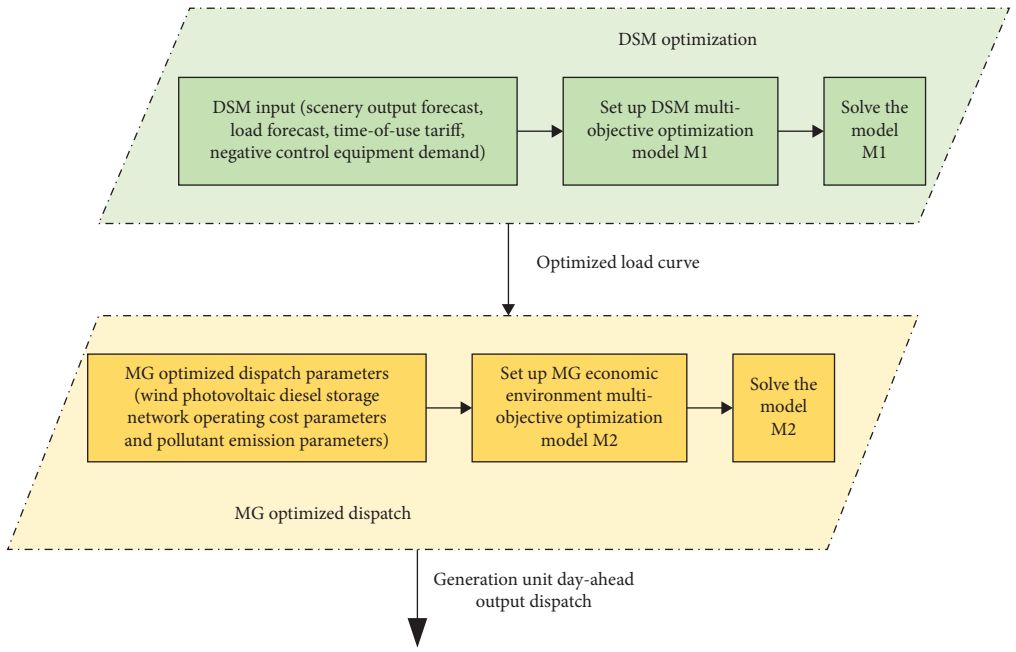

Figure 2: MG scheduling model framework.

4. Multimodal Multiobjective Optimization Solution Model Based on the Local Convergence Index

Many engineering applications in the real-world often require the consideration of multiple optimization objectives. Usually, the different objectives are mutually constrained and can only be traded off to obtain a satisfactory solution for the decision maker. Multiobjective optimization problems (MOPs) can be represented as follows:

$$\begin{aligned} \min O(i) &= \{o_1(i), o_2(i), \cdots, o_w(i)\}, \\ \text{s. n. } i &= (i_1, i_2, \cdots, i_t) \in \Omega, \end{aligned} \tag{25}$$

where Ω is the feasible domain of the problem and $o_w(i)$ is the i-th objective function value of the decision vector. Unlike a single-objective optimization problem with a single global optimum, in a multiobjective optimization problem, there are multiple nondominated solutions, which are called Pareto optimal solution sets. The solution i_G dominates the solution i_H when and only when

$$\begin{cases} \forall x \in 1, 2, \cdots, w, o_x(i_G) \le o_x(i_H), \\ \exists y \in 1, 2, \cdots, w, o_y(i_G) < o_y(i_H). \end{cases} \tag{26}$$

In general, multiobjective evolutionary algorithms (MOEAs) give a set of mutually exclusive solution sets, called Pareto solution set (PS). Also, the mapping of PS on the objective space is called Pareto optimal front (PF).

4.1. Local Convergence Metrics. Traditional MOEAs focus more on the convergence of the solution set, so most algorithms choose convergence as the first criterion for the selection of offspring individuals. The multimodal multiobjective optimization algorithms designed based on traditional MOEAs are taken into account of the diversity of decision spaces and therefore can obtain more equivalent PSs. However, traditional algorithms tend to focus only on obtaining global PSs, thus discarding the search for local PSs. In order to enhance the search capability of the algorithm for local PS, a local convergence index is proposed by referring to the meta-adaptation value proposed in the SPEA2 algorithm [29]. This paper emphasizes local Pareto optimal solutions and provides guidance for selecting parent individuals by calculating a local convergence index X_{LC}^x for each solution. For the solution i_x, the local convergence index is calculated as follows:

$$X_{\mathrm{LC}}^x = \sum_{y \in T_x} S_y D_{y,x}, \tag{27}$$

where M_x denotes the number of neighboring solutions of solution i_x. $D_{y,x} \in \{0, 1\}$, where $D_{y,x} = 1$ denotes the solution i_xPareto-dominated solution. When $X_{\mathrm{LC}}^x = 0$, it means that solution i_x is not dominated by any of its neighboring solutions, that is, solution i_x is locally Pareto optimal. S_x denotes the number of times that solution i_x Pareto dominates its neighboring solutions. The larger the value of S_x, the better the relative performance of solution i_x. The specific calculation procedure is as follows:

$$S_x = \sum_{y \in T_x} D_{x,y}. \tag{28}$$

Figure 3 shows a schematic diagram of the calculation of the local convergence metric proposed in this paper. Unlike the SPEA2 algorithm, the meta-adaptation value needs to be compared with all the individuals in the population. In the calculation of the local convergence index, individuals are only compared with their own neighboring solutions to improve the convergence of the local optimal solution. Specifically, for solution G in the decision space, it is in the local PS (circle region). In traditional MOEAs, solutions G

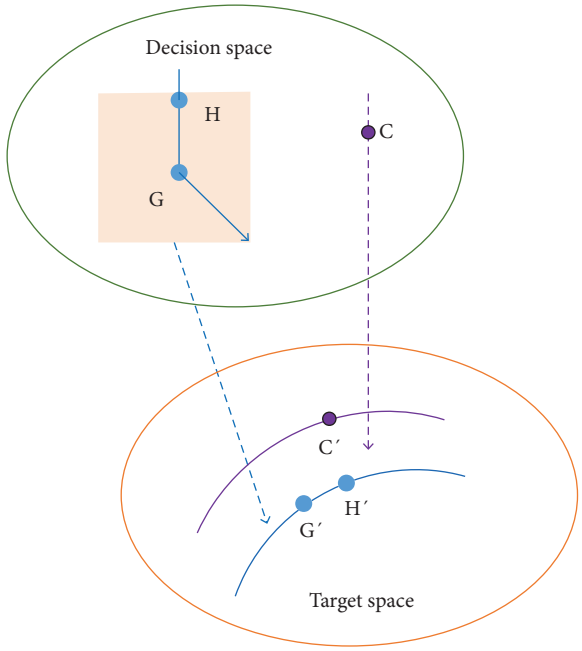

Figure 3: Schematic diagram of local convergence index.

and H, located in the global PS (where point C is situated), are dominated by C, leading to their exclusion from the evolutionary process. In the calculation of the local convergence index, solution G is compared with its own neighboring solutions (in the current schematic, only solution H is a neighbor) in the calculation of the dominance relation. In this case, solution G is a nondominated solution, which can be retained and successfully proceed to the next evolution. The concept of neighbors is used in the calculation of the local convergence index, and the definition of neighboring solutions in the decision space is subjective and requires the introduction of parameters. In this paper, two solutions i_x and i_y are called neighbors when and only when their Euclidean distance is less than Q. The calculation is as follows:

$$Q = \frac{1}{2}\left(\prod_{d=1}^{D}\left(i_d^{\max} - i_d^{\min}\right)\right)^{(1/D)}, \tag{29}$$

where D denotes the number of decision variables. $i_d^{\max}$ and $i_d^{\min}$ represent the maximum and minimum values of the d-th decision variable, respectively.

4.2. Algorithmic Framework. Based on the local convergence indicator, a multimodal multiobjective evolutionary algorithm (MMEA based on local convergence indicator, X_{LC}-MMEA) is proposed in this paper. The algorithmic framework of X_{LC}-MMEA is represented by algorithm 1. Like most MOEAs, X_{LC}-MMEA consists of the following steps: population initialization, mating selection, offspring generation, and environment selection. The study introduces a local convergence index to identify global and local Pareto solutions. This index is employed as a binary competition criterion in selecting parent individuals, accelerating the algorithm's convergence and enhancing local exploration capability. Specifically, two solutions are randomly selected from the current population and their local convergence index values are compared. If their local convergence metrics are the same, the one with the smaller crowding distance is selected. This process will be repeated until N individuals are selected. After that, the selected parent individuals will generate progeny using SBX and polynomial mutation (PM). Figure 4 shows the flow diagram of algorithm 1.

4.3. Environment Selection Strategy. In this paper, a new environment selection strategy is designed for the search problem of local PS. The environment selection strategy utilizes the crowding distance as a second criterion, considering both the decision space and target space. It helps in selecting individuals that contribute to a uniformly distributed solution set. In this section, the ILC-based environment selection strategy is discussed in detail, and the basic idea is represented by algorithm 2 (see Figure 5).

X_{LC}-MMEA uses the crowding distance as a second criterion to select individuals in the population. In general, traditional MOEAs focus more on the uniformity of the solution set distribution in the target space, while the proposed algorithm focuses more on the uniformity of the decision space. This can be illustrated by the distribution of the target space and decision space in Figure 6.

The left portion of Figure 6 illustrates that the solution is optimally dispersed across the decision space, albeit suboptimally dispersed in the objective space, aligning with conventional multimodal evolutionary algorithms (MMEAs). Conversely, the central part of Figure 6 indicates that the solution is inadequately distributed in the decision space but is optimally distributed in the objective space, mirroring traditional multiobjective evolutionary algorithms (MOEAs). The quintessential state for solution distribution, depicted on the right side of Figure 6, entails the solution being optimally dispersed in both the decision and objective spaces. To realize this objective, an enhanced method for computing the population crowding distance is delineated hereinafter.

$$\mathrm{CD}_x = \frac{M-1}{\sum_{y=1,y\neq x}^{M}\left(1/\left\|\mathbf{i}_y - \mathbf{i}_x\right\|\right)} + \frac{M-1}{\sum_{y=1,y\neq x}^{M}\left(1/\left\|o\left(\mathbf{i}_y\right) - o\left(\mathbf{i}_x\right)\right\|\right)}, \tag{30}$$

where $\|i_y - i_x\|$ denotes the Euclidean distance between i_x and i_y. $o(i_x)$ represents the normalized value of the target vector corresponding to the solution i_x. Before the calculation, the values of i_x and i_y need to be normalized. The new crowded distance considers the solution set's relative positions in both target and decision spaces, ensuring

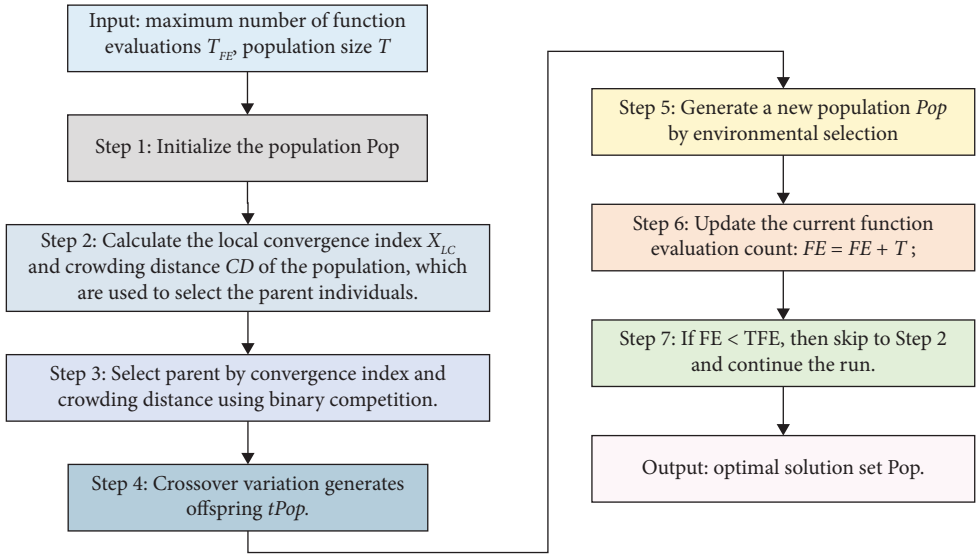

Figure 4: Framework diagram of the X_{LC}-MMEA algorithm.

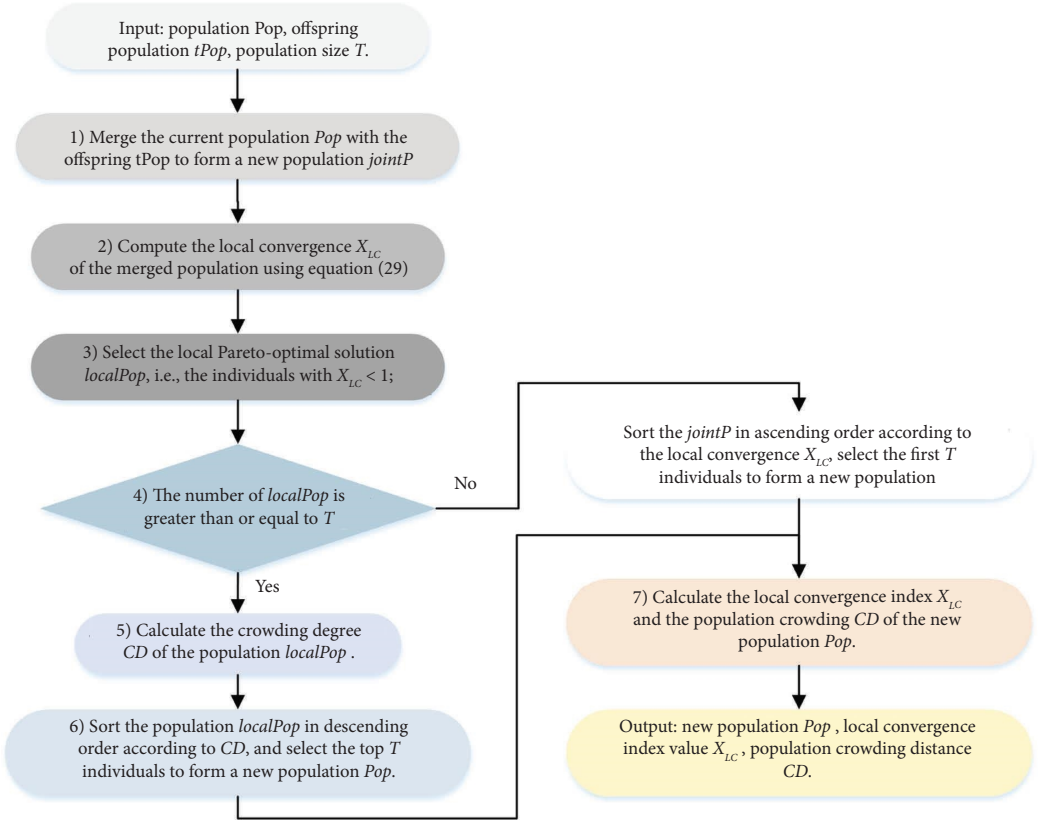

Figure 5: Flowchart of environment selection strategy.

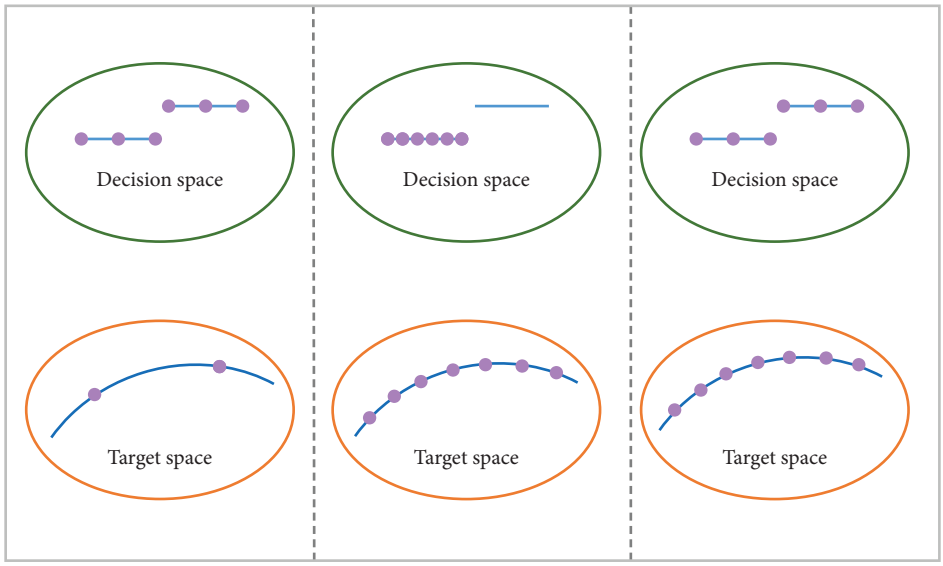

Figure 6: Uniformity of the distribution of the target space and decision space.

a more uniform distribution across both. In addition, in order to better balance the differences between the two spaces, the algorithm uses a uniform normalization strategy for the vectors in both spaces.

5. Result Analysis and Discussion

In the experiments, a typical MG structure is used in this paper. This MG structure includes elements, such as wind turbines, photovoltaic generation, and controllable loads. The specification of this test network includes the capacity, initial state, connection mode, and power consumption requirements of each element in the MG.

5.1. Comparative Analysis of Different Dispatching Cases. To validate the models and methods delineated in this paper, three MG dispatching scenarios are conceptualized, utilizing a typical MG structure as the research arithmetic: (1) development of an MG dispatching model without accounting for DSM; (2) formulation of a DSM optimization model to optimize the load with the aim of minimizing the customer's electricity procurement cost, followed by the construction of an MG dispatching model; and (3) formulation of a DSM multiobjective optimization model, followed by the development of an MG dispatching model, and resolving the model utilizing a multimodal multiobjective optimization algorithm.

The study incorporates the load under different scenarios: without DSM optimization, with DSM single-objective optimization, and with DSM multiobjective optimization, into the MG economic environment dispatching model to provide a detailed analysis. The utilization of new energy output is visually represented in Figure 7. As discernible from Figure 7, the utilization rate of new energy output is diminished in the absence of DSM optimization owing to the discord between the timing and magnitude of new energy output and load demand. Owing to the substantial quantity of "abandoned wind and light," the traditional DG output and the aggregate amount of electricity procured by the MG from the grid are considerably elevated. The economic implications are significant, as the MG incurs higher costs in procuring electricity from the grid and relies more heavily on conventional energy sources. This translates into increased operational costs and potentially higher greenhouse gas emissions due to greater dependence on nonrenewable energy. Introducing single-objective DSM optimization brings about substantial improvements in MG performance. The introduction of single-objective DSM optimization can significantly improve MG performance by introducing DSM multiobjective optimization for both economic and environmental goals. This plan makes more efficient use of energy and reduces costs, while significantly reducing carbon emissions and environmental impact. With the help of DSM, MG is able to utilize new energy sources more efficiently and reduce its reliance on conventional power generation, thereby reducing carbon emissions and environmental impact.

5.2. Comparative Analysis of Different Algorithms. In this section, the load data of a typical daytime in summer and winter in a region are selected to test the MG economic environmental dispatch model. Literature [30], literature [31], and the proposed algorithm are used to solve the model. The operating cost, power purchase cost, environmental cost, and single-day integrated cost of the MG are compared, and the calculation results of the three algorithms are shown in Table 1. The integrated energy satisfaction, PV consumption rate, and electricity autonomy rate of the system at the optimal solution are also analyzed, and various indicators are shown in Figure 8.

In Table 1, the optimization results for the MG economic environmental dispatch model during a typical summer and winter day are presented. The proposed algorithm consistently outperforms literature [30] and literature [31] in terms

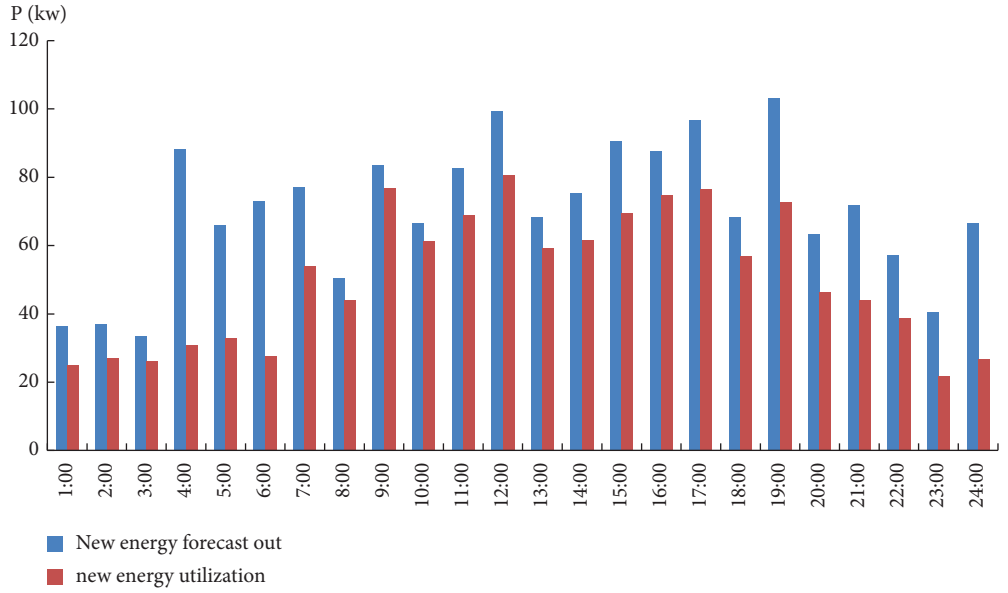

(a)

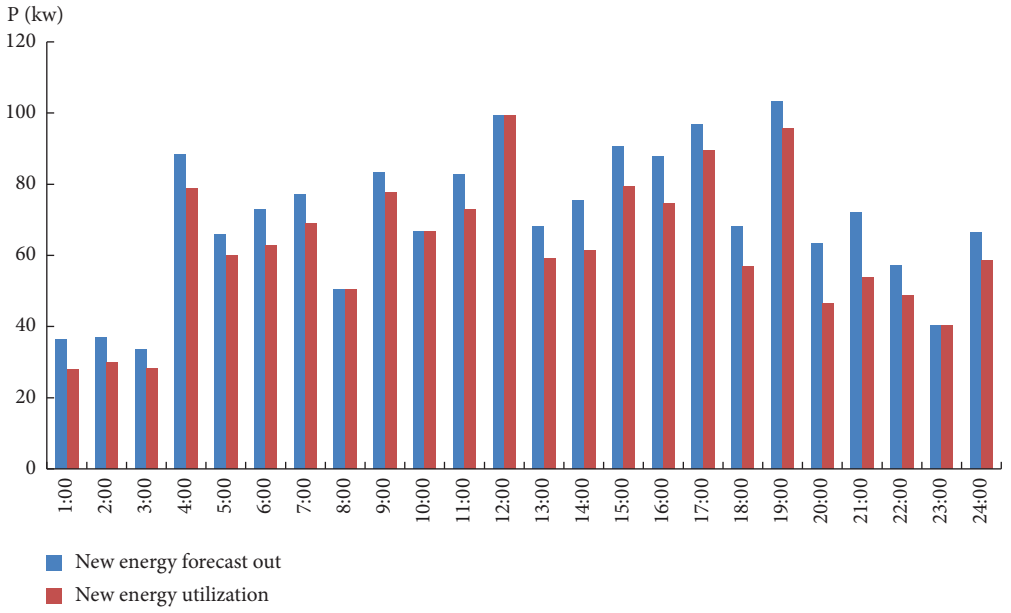

(b)

Figure 7: Continued.

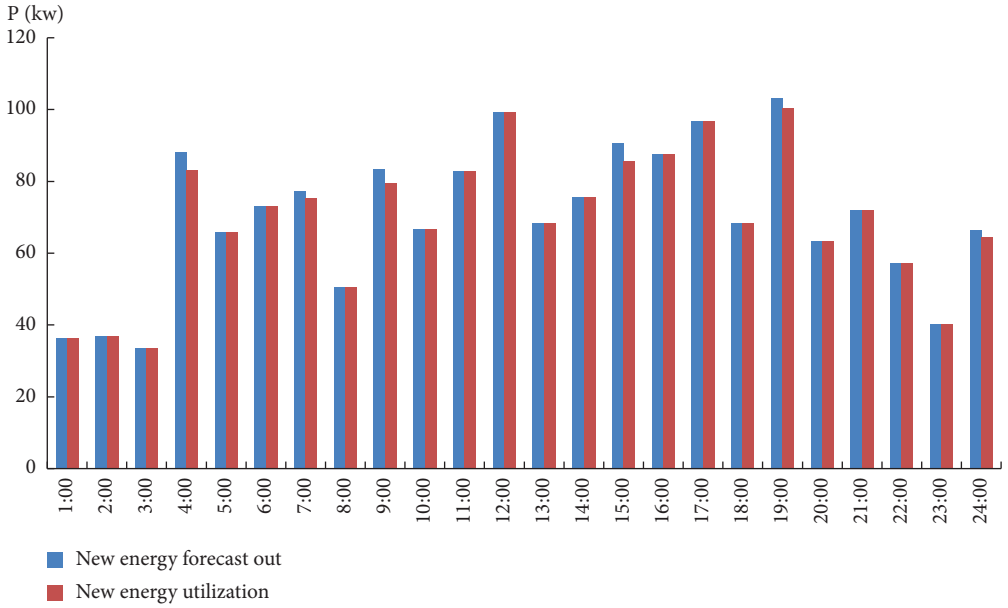

Figure 7: New energy utilization. (a) No DSM optimization. (b) DSM single-objective optimization. (c) DSM multiobjective optimization.

Table 1: Objective function optimization of the integrated energy system.

	Category	Literature [30]	Literature [31]	Proposed
Summer	Operating cost	5104.6	5994.2	4168.2
	Power purchase cost	7151.4	5887.4	4586.7
	Environmental cost	33.2	49.1	52.4
	Single day integrated cost	5089.5	5332.3	3839.2
Winter	Operating cost	3211.9	4286.3	2974.5
	Power purchase cost	4830.2	4340.4	3300.3
	Environmental cost	78.8	93.1	101.7
	Single day integrated cost	3277.6	3849.5	2745.9

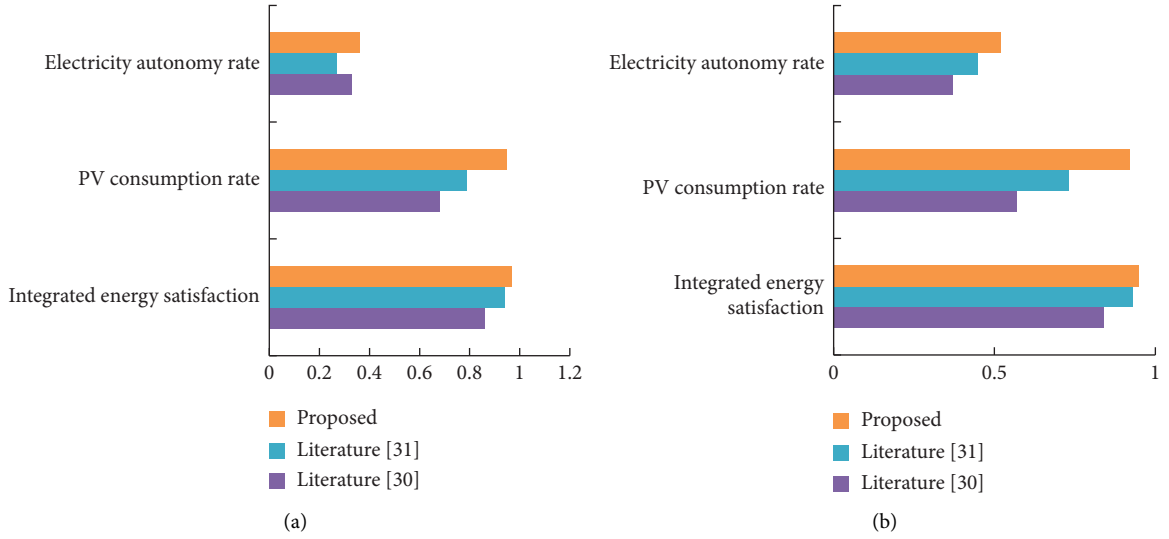

Figure 8: Performance index evaluation of MG scheduling model. (a) Summer. (b) Winter.

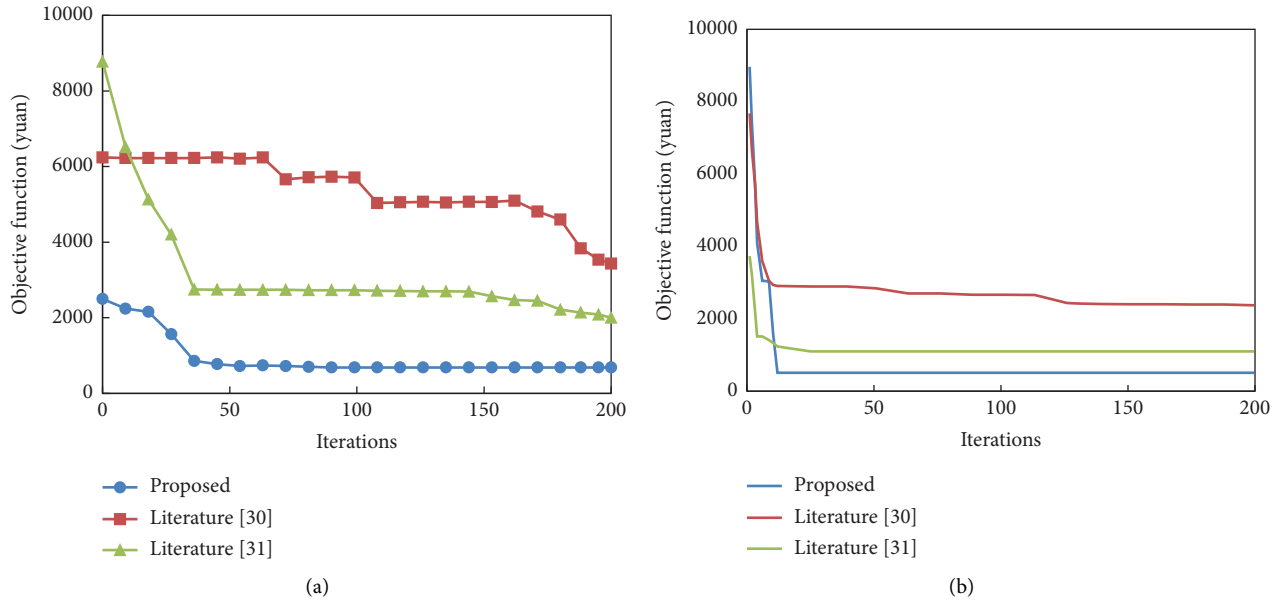

Figure 9: Convergence curves of the 3 algorithms. (a) Summer optimal solution. (b) Winter optimal solution.

of integrated cost, showcasing its effectiveness. During summer, the integrated cost achieved by the proposed algorithm is notably 32.6% and 38.9% lower than literature [30] and literature [31], respectively. In winter, the reduction is even more pronounced, with a 19.4% and 40.2% improvement over literature [30] and literature [31]. While the operating and power purchase costs decrease significantly, there is a slight increase in environmental cost. This tradeoff is crucial for achieving a balance between economic efficiency and environmental sustainability.

Figure 8 provides a comprehensive evaluation of the MG scheduling model's performance. The proposed algorithm achieves a higher integrated energy satisfaction of load users (0.97 and 0.95 for the two typical days), indicating an efficient utilization of available energy resources. Moreover, the average PV consumption rate of the proposed algorithm is 23% and 49.6%, which is significantly higher than literature [30] and literature [31], demonstrating the algorithm's efficacy in harnessing solar energy. The electricity autonomy rates are 0.36 and 0.52. Although only slightly better, it signifies the system's ability to operate independently. These results affirm that the proposed algorithm not only minimizes costs but also enhances the satisfaction of energy demand while maintaining environmental benefits.

Three algorithms are used simultaneously to optimally solve the MG economic environment dispatch model at two typical day times under the same operating conditions. The maximum number of iterations in the algorithm is 200, and the search population is 30 (see Figure 9). From Figure 9, it can be seen that in summer and winter time, the algorithm of this paper has fewer computational results than the literature [30] and literature [31], and the number of iterations used to converge to the optimal solution is the least. In summer, the proposed algorithm achieves the optimal solution at the 90th iteration, while the algorithms in literature [30] and literature [31] only find the local optimal solution in the whole process. In winter, the proposed algorithm achieves the optimal solution at the 15th iteration, and the algorithm in literature [31] falls into the local optimal solution at the 6th generation until the end of the solving process. The algorithm of literature [30] keeps jumping from the local solution to a better local solution but does not find the optimal solution. The convergence accuracy, solution speed, and global search capability of the algorithm in this paper show obvious superiority.

The experimental results depicted in Figure 9 underscore the superior convergence efficiency and accuracy of the proposed algorithm in comparison to literature [30] and literature [31]. In both summer and winter scenarios, the algorithm of this paper demonstrates a notable reduction in computational iterations required to reach the optimal solution. During summer, the algorithm achieves global optimality at the 90th iteration, while the algorithms in literature [30] and literature [31] only find the local optimal solution in the whole process. It stands in stark contrast to the local optima found in literatures [30, 31]. In winter, the proposed algorithm converges to the optimal solution at the 15th iteration, outperforming literature [31], which remains trapped in a local optimum. The algorithm of literature [30] keeps jumping from the local solution to a better local solution but does not find the optimal solution. The proposed algorithm's advantages include high convergence accuracy, swift solution speed, and superior global search capability. These characteristics make it a robust and efficient tool for optimizing microgrid operations, especially in dynamic and time-sensitive scenarios, affirming its practical applicability in real-world energy management.

Figure 10 visually displays the curves of all algorithms on problems with PS. As can be seen from Figure 10, the proposed method is able to find both global and local PSs of the problem, and the obtained PF distribution is more uniform. This is because the method introduces a new way of

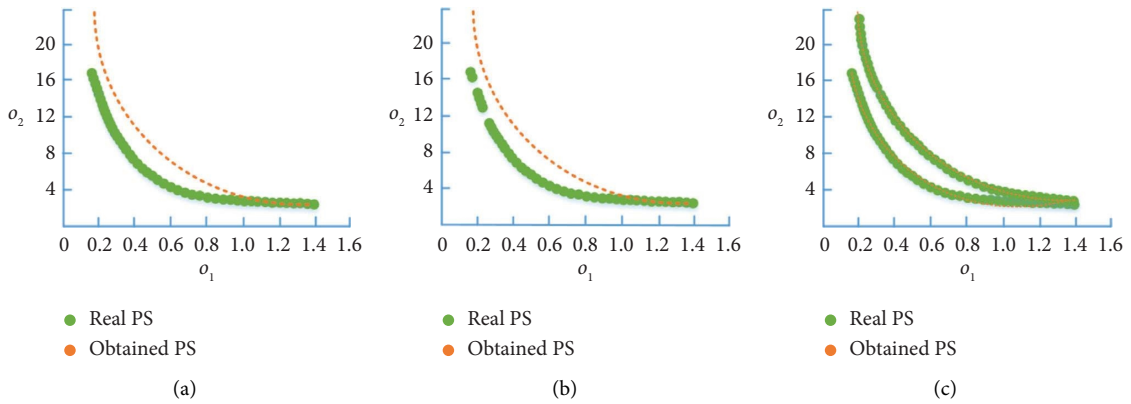

Figure 10: Performance of different algorithms on global and local problems. (a) Literature [30]. (b) Literature [31]. (c) Proposed.

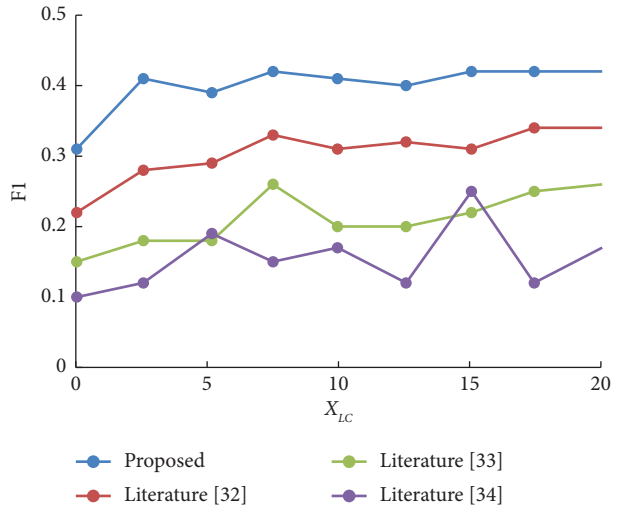

Figure 11: Influence of X_{LC} value on $F1$ index.

calculating population crowding, which can better balance the uniformity of the distribution in the target space and the decision space.

5.3. Sensitivity Analysis of Local Convergence Index. The algorithms are compared with the current state-of-the-art algorithms (literature [32], literature [33], and literature [34]) in terms of F1 for different X_{LC} values. The comparison results are shown in Figure 11.

From Figure 11, it can be seen that when the X_{LC} value is small, the $F1$ value of this paper's algorithm at different values is higher than the other compared algorithms. Moreover, the selection of different X_{LC} values for this paper's algorithm has less impact on the algorithm's detection results. The results from the sensitivity analysis clearly indicate the robustness and adaptability of the proposed algorithm across diverse operating conditions.

6. Conclusion

In this study, a multiobjective optimization methodology for a new energy MG incorporating DSM is devised, with a focus on the primary objectives of minimizing the operational cost of the MG system and reducing the environmental impact. Initially, a DSM optimization model is developed, emphasizing load shifting in controllable devices while considering the utilization rate of new energy, electricity procurement costs for customers, and load leveling. Subsequently, an MG scheduling model is formulated to incorporate both economic and environmental protection objectives. Eventually, the experimental conclusions are as follows: (1) quantitative analysis: the comparative experimental results of different scheduling cases prove that the DSM multiobjective optimization in this paper can save economic costs more effectively and at the same time greatly reduce carbon emissions and the impact on the environment. (2) Qualitative analysis: in the summer, the proposed algorithm achieves an integrated cost that is 32.6% and 38.9% lower than that of literature [30] and literature [31], respectively. In the winter, the proposed algorithm achieves integrated costs 19.4% and 40.2% lower than literature [30] and literature [31], respectively. Moreover, our multimodal multiobjective optimization solution model, based on the local convergence index, is a flexible framework that can be fine-tuned to address the specific needs and constraints of different MGs or regions. The local convergence index allows

us to efficiently find global and local Pareto optimal solutions, making it easier to tailor our methodology to diverse scenarios.

However, the methodology in this paper may not take into account all types of controllable devices and their different characteristics. Adaptive control strategies that can be adaptively tuned to the specific characteristics and requirements of newly introduced devices will be further investigated in the future to ensure wider applicability. Furthermore, due to its complexity, it is challenging to implement the algorithm in real-world MGs. In particular, external factors, such as numerous controllable devices, different load profiles, and weather need to be taken into account. Future research will customize the algorithm for different real-world MG scenarios so that it can be seamlessly integrated into multiple environments.

Data Availability

The labeled data set used to support the findings of this study is available from the corresponding author upon request.

Conflicts of Interest

The authors declare that they have no conflicts of interest.

Acknowledgments

This work was supported by the 2023-2024 Jiangsu Vocational Education Research Project+Research on the Development and Sharing of Digital Resource Database in Vocational Colleges (Grant No. XHYBLX2023285).

References

[1] L. Li, J. Lin, N. Wu et al., "Review and outlook on the international renewable energy development," *Energy and Built Environment*, vol. 3, no. 2, pp. 139–157, 2022.

[2] S. I. Khattak, M. Ahmad, Z. U. Khan, and A. Khan, "Exploring the impact of innovation, renewable energy consumption, and income on CO2 emissions: new evidence from the BRICS economies," *Environmental Science and Pollution Research*, vol. 27, no. 12, pp. 13866–13881, 2020.

[3] G. He, J. Lin, Y. Zhang et al., "Enabling a rapid and just transition away from coal in China," *One Earth*, vol. 3, no. 2, pp. 187–194, 2020.

[4] A. D. W. M. Sidik and Z. Akbar, "Analyzing the potential for utilization of new renewable energy to support the electricity system in the cianjur regency region," *Fidelity: Jurnal Teknik Elektro*, vol. 3, no. 3, pp. 46–51, 2021.

[5] C. Ghenai, T. Salameh, and A. Merabet, "Technico-economic analysis of off grid solar PV/Fuel cell energy system for residential community in desert region," *International Journal of Hydrogen Energy*, vol. 45, no. 20, pp. 11460–11470, 2020.

[6] O. Krishan and S. Suhag, "An updated review of energy storage systems: classification and applications in distributed generation power systems incorporating renewable energy resources," *International Journal of Energy Research*, vol. 43, no. 12, pp. 6171–6210, 2019.

[7] U. Yilmaz and O. Turksoy, "Artificial intelligence based active and reactive power control method for single-phase grid connected hydrogen fuel cell systems," *International Journal of Hydrogen Energy*, vol. 48, no. 21, pp. 7866–7883, 2023.

[8] H. Lotfi and R. Ghazi, "Optimal participation of demand response aggregators in reconfigurable distribution system considering photovoltaic and storage units," *Journal of Ambient Intelligence and Humanized Computing*, vol. 12, no. 2, pp. 2233–2255, 2021.

[9] A. M. Hussien, H. M. Hasanien, and S. F. Mekhamer, "Sunflower optimization algorithm-based optimal PI control for enhancing the performance of an autonomous operation of a microgrid," *Ain Shams Engineering Journal*, vol. 12, no. 2, pp. 1883–1893, 2021.

[10] F. Moghateli, S. A. Taher, A. Karimi, and M. Shahidehpour, "Multi-objective design method for construction of multi-microgrid systems in active distribution networks," *IET Smart Grid*, vol. 3, no. 3, pp. 331–341, 2020.

[11] H. Lotfi and A. A. Shojaei, "A dynamic model for multi-objective feeder reconfiguration in distribution network considering demand response program," *Energy Systems*, vol. 14, no. 4, pp. 1051–1080, 2022.

[12] X. Wang, J. Atkin, N. Bazmohammadi, S. Bozhko, and J. M. Guerrero, "Optimal load and energy management of aircraft microgrids using multi-objective model predictive control," *Sustainability*, vol. 13, no. 24, Article ID 13907, 2021.

[13] L. Bhamidi and S. Sivasubramani, "Optimal planning and operational strategy of a residential microgrid with demand side management," *IEEE Systems Journal*, vol. 14, no. 2, pp. 2624–2632, 2020.

[14] K. Dehghanpour and H. Nehrir, "Real-time multiobjective microgrid power management using distributed optimization in an agent-based bargaining framework," *IEEE Transactions on Smart Grid*, vol. 9, no. 6, pp. 6318–6327, 2018.

[15] H. Zhang, D. Yue, C. Dou, and G. P. Hancke, "PBI based multi-objective optimization via deep reinforcement elite learning strategy for micro-grid dispatch with frequency dynamics," *IEEE Transactions on Power Systems*, vol. 38, no. 1, pp. 488–498, 2023.

[16] Z. Younes, I. Alhamrouni, S. Mekhilef, and M. J. A. S. E. J. Reyasudin, "A memory-based gravitational search algorithm for solving economic dispatch problem in micro-grid," *Ain Shams Engineering Journal*, vol. 12, no. 2, pp. 1985–1994, 2021.

[17] W. Zhu, J. Guo, G. Zhao, and B. Zeng, "Optimal sizing of an island hybrid microgrid based on improved multi-objective grey wolf optimizer," *Processes*, vol. 8, no. 12, p. 1581, 2020.

[18] M. Vosoogh, M. Rashidinejad, A. Abdollahi, and M. Ghaseminezhad, "An intelligent day ahead energy management framework for networked microgrids considering high penetration of electric vehicles," *IEEE Transactions on Industrial Informatics*, vol. 17, no. 1, pp. 667–677, 2021.

[19] Z. H. A. Al-Tameemi, T. T. Lie, G. Foo, and F. Blaabjerg, "Optimal coordinated control of DC microgrid based on hybrid PSO–GWO algorithm," *Electricity*, vol. 3, no. 3, pp. 346–364, 2022.

[20] M. Ghiasi, "Detailed study, multi-objective optimization, and design of an AC-DC smart microgrid with hybrid renewable energy resources," *Energy*, vol. 169, no. C, pp. 496–507, 2019.

[21] M. Ghiasi, T. Niknam, M. Dehghani, P. Siano, H. Haes Alhelou, and A. Al-Hinai, "Optimal multi-operation energy management in smart microgrids in the presence of ress based on multi-objective improved de algorithm: cost-emission based optimization," *Applied Sciences*, vol. 11, no. 8, p. 3661, 2021.

[22] M. Ghiasi, T. Niknam, M. Dehghani et al., "Multipurpose FCS model predictive control of VSC-based microgrids for islanded and grid-connected operation modes," *IEEE Systems Journal*, vol. 17, no. 2, pp. 2558–2569, 2023.

[23] F. Mohamad, J. Teh, C. M. Lai, and L. R. Chen, "Development of energy storage systems for power network reliability: a review," *Energies*, vol. 11, no. 9, p. 2278, 2018.

[24] N. Hatziargyriou, A. Dimeas, N. Vasilakis, D. Lagos, and A. Kontou, "The kythnos microgrid: a 20-year history," *IEEE Electrification Magazine*, vol. 8, no. 4, pp. 46–54, 2020.

[25] X. Yan and W. Zhang, "Review of VSG control-enabled universal compatibility architecture for future power systems with high-penetration renewable generation," *Applied Sciences*, vol. 9, no. 7, p. 1484, 2019.

[26] H. Lotfi, "Multi-objective energy management approach in distribution grid integrated with energy storage units considering the demand response program," *International Journal of Energy Research*, vol. 44, no. 13, pp. 10662–10681, 2020.

[27] W. Tao, M. Ma, M. Ding, W. Xie, and C. Fang, "A priority-based synchronous phasor transmission protocol extension method for the active distribution network," *Applied Sciences*, vol. 9, no. 10, p. 2135, 2019.

[28] A. T. Meshram, A. V. Vanalkar, K. B. Kalambe, and A. M. Badar, "Pesticide spraying robot for precision agriculture: a categorical literature review and future trends," *Journal of Field Robotics*, vol. 39, no. 2, pp. 153–171, 2022.

[29] X. Liu and D. Zhang, "An improved SPEA2 algorithm with local search for multi-objective investment decision-making," *Applied Sciences*, vol. 9, no. 8, p. 1675, 2019.

[30] M. Abdelsalam, H. Y. Diab, and A. A. El-Bary, "A meta-heuristic Harris hawk optimization approach for coordinated control of energy management in distributed generation based Microgrids," *Applied Sciences*, vol. 11, no. 9, p. 4085, 2021.

[31] Y. Wang, F. Li, H. Yu et al., "Optimal operation of microgrid with multi-energy complementary based on moth flame optimization algorithm," *Energy Sources, Part A: Recovery, Utilization, and Environmental Effects*, vol. 42, no. 7, pp. 785–806, 2020.

[32] D. Dinh-Cong and T. Nguyen-Thoi, "An effective damage identification procedure using model updating technique and multi-objective optimization algorithm for structures made of functionally graded materials," *Engineering with Computers*, vol. 39, no. 2, pp. 1229–1247, 2023.

[33] J. O. Agushaka, A. E. Ezugwu, and L. Abualigah, "Gazelle optimization algorithm: a novel nature-inspired meta-heuristic optimizer," *Neural Computing and Applications*, vol. 35, no. 5, pp. 4099–4131, 2023.

[34] F. K. Karim, D. S. Khafaga, M. M. Eid, S. K. Towfek, and H. K. Alkahtani, "A novel bio-inspired optimization algorithm design for wind power engineering applications time-series forecasting," *Biomimetics*, vol. 8, no. 3, p. 321, 2023.